BAFF Attenuates Immunosuppressive Monocytes in the Melanoma Tumor Microenvironment

Wei Liu[1], Paweł Stachura[1], Haifeng C. Xu[1], Renáta Váraljai[2], Prashant Shinde[1], Nikkitha Umesh Ganesh[1], Matthias Mack[3], Anke Van Lierop[4], Anfei Huang[1], Balamurugan Sundaram[1], Karl S. Lang[5], Daniel Picard[6,7,8,9], Ute Fischer[6], Marc Remke[6,7,8,9], Bernhard Homey[4], Alexander Roesch[2], Dieter Häussinger[10], Philipp A. Lang[1], Arndt Borkhardt[6], and Aleksandra A. Pandyra[6]

ABSTRACT

Emerging evidence indicates B-cell activating factor (BAFF, *Tnfsf13b*) to be an important cytokine for antitumor immunity. In this study, we generated a BAFF-overexpressing B16.F10 melanoma cell model and found that BAFF-expressing tumors grow more slowly *in vivo* than control tumors. The tumor microenvironment (TME) of BAFF-overexpressing tumors had decreased myeloid infiltrates with lower PD-L1 expression. Monocyte depletion and anti-PD-L1 antibody treatment confirmed the functional importance of monocytes for the phenotype of BAFF-mediated tumor growth delay. RNA sequencing analysis confirmed that monocytes isolated from BAFF-overexpressing tumors were characterized by a less exhaustive phenotype and were enriched for in genes involved in activating adaptive immune responses and

NF-κB signaling. Evaluation of patients with late-stage metastatic melanoma treated with inhibitors of the PD-1/PD-L1 axis demonstrated a stratification of patients with high and low BAFF plasma levels. Patients with high BAFF levels experienced lower responses to anti-PD-1 immunotherapies. In summary, these results show that BAFF, through its effect on tumor-infiltrating monocytes, not only impacts primary tumor growth but can serve as a biomarker to predict response to anti-PD-1 immunotherapy in advanced disease.

Significance: The BAFF cytokine regulates monocytes in the melanoma microenvironment to suppress tumor growth, highlighting the importance of BAFF in antitumor immunity.

Introduction

B-cell activating factor (BAFF), a member of the tumor necrosis factor (TNF) family, is a cytokine critical for B-cell development and survival (1). Produced by myeloid cells (2), malignant B cells (3), activated T cells (4), and bone marrow stromal cells (5), BAFF exerts its biological functions through binding with high affinity to

the BAFF, TACI, and BCMA receptors (6, 7) and affects aspects of B-cell development, maintenance, and survival. Elevated BAFF levels have been observed in patients with autoimmune diseases (8, 9). The functional significance of elevated BAFF in autoimmune diseases has led to the development of anti-BAFF mAbs such as belimumab already approved for the treatment of systemic lupus erythematosus (10). Emerging evidence indicates that BAFF regulates immune cells other than B cells. BAFF-R is expressed on activated, central, and effector memory T cells (11) as well as monocytes (12). Taken together, BAFF is a cytokine of clinical importance in autoimmune diseases and is involved in various aspects of B-cell function but has also been shown to affect T cells and innate immune cells.

In addition to its recognized role in autoimmune diseases, there are reports indicating BAFF to be associated with hematologic malignancies where patients have been shown to have elevated serum BAFF levels that negatively correlated with clinical outcome (13). The above findings are not surprising given that BAFF is a survival factor for normal B cells and would therefore also sustain the proliferation of malignant B cells. In solid tumors however, the pathophysiologic link between BAFF and cancer is tenuous. Although elevated serum BAFF levels were observed in patients with neuroendocrine tumors (14), BAFF expression did not differ between normal and cancerous tissue in patients with breast cancer (15). BAFF serum levels were shown to be higher in patients with pancreatic ductal adenocarcinoma where BAFF promoted tumor invasion and metastasis (16). When considering individual contributions of BAFF–affected immune cells to antitumor immunity, BAFF derived from dendritic cells improved antitumor efficacy (17) and loss of BAFF production in the epithelium led to prostate tumor escape from immunosurveillance (18). Importantly, Yarchoan and colleagues have recently shown that *in vitro* BAFF treatment upregulated multiple B-cell costimulatory molecules, and when

[1]Department of Molecular Medicine II, Medical Faculty, Heinrich-Heine University, Düsseldorf, Germany. [2]Department of Dermatology, University Hospital Essen, West German Cancer Center, University of Duisburg-Essen and the German Cancer Consortium (DKTK), Essen, Germany. [3]Department of Nephrology, Universitätsklinikum Regensburg, Regensburg, Germany. [4]Department of Dermatology, Medical Faculty, Heinrich-Heine University, Düsseldorf, Germany. [5]Institute of Immunology, Medical Faculty, University of Duisburg-Essen, Essen, Germany. [6]Department of Pediatric Oncology, Hematology and Clinical Immunology, Medical Faculty, Center of Child and Adolescent Health, Heinrich-Heine-University, Düsseldorf, Germany. [7]Division of Pediatric Neuro-Oncogenomics, German Cancer Research Center (DKFZ), Heidelberg, Germany. [8]German Consortium for Translational Cancer Research (DKTK), partner site Essen/Düsseldorf, Düsseldorf, Germany. [9]Department of Neuropathology, Medical Faculty, Heinrich-Heine University, Düsseldorf, Germany. [10]Department of Gastroenterology, Hepatology, and Infectious Diseases, Medical Faculty, Heinrich-Heine University, Düsseldorf, Germany.

Corresponding Author: Aleksandra A. Pandyra, Department of Pediatric Oncology, Hematology and Clinical Immunology, Medical Faculty, Center of Child and Adolescent Health, Heinrich-Heine-University, Universitätsstraβe 1, Düsseldorf, 40225, Germany. E-mail: aleksandra.pandyra@uni-duesseldorf.de

administered systemically at high doses in tumor-bearing mice, had multiple immunoregulatory functions (19) including an accumulation of B cells and FOXP3$^+$ T regulatory cells (Tregs) in the spleen. When the authors mined data from The Cancer Genome Atlas (TCGA) they found that higher BAFF expression was associated with improved 5-year survival although it is difficult to conclude whether the survival was based on higher BAFF expression in the tumor or in infiltrates that are likely to be a source of BAFF (19). Although the role of BAFF in hematologic malignancies is better established, less is known about its prognostic or functional role in solid tumors, although it is clear that BAFF is an important emerging cytokine involved in antitumor immunity.

To specifically examine the effects of local BAFF within the tumor microenvironment (TME), we generated BAFF-overexpressing murine melanoma cell lines. We investigated their ability to impact primary tumor growth using knockout murine models and depletion antibodies and found that intratumoral BAFF critically affects the number of tumor-infiltrating monocytes and their immunosuppressive phenotype.

Materials and Methods

Cell culture and compounds

RMA/S and HEK293T cells were cultured and obtained as previously described (20). B16.F10.gp33 (B16.gp33) were provided by Dr. H.P. Pircher, Freiburg, and cultured as described previously (21). Cell lines were maintained DMEM supplemented with 10% FBS (GIBCO), penicillin, and streptomycin. Cells routinely tested negative for mycoplasma, last tested August 2021 (MB, Minerva Biolabs). Cells were used for a maximum of five passages from time of thawing.

Mice

$JHt^{-/-}$, $Cd8^{-/-}$, $Ifng^{-/-}$ and $Baffr^{-/-}$ mice were bred in a C57BL/6 background and maintained under specific pathogen-free conditions. Tumors were measured using calipers and tumor volume was calculated using the following formula: (tumor length $\times$ width^2)/2. Experiments were approved under the authorization of the LANUV in accordance with German law for animal protection.

Patient samples

Plasma from 11 healthy donor volunteers was collected at University Hospital Düsseldorf, Department of Molecular Medicine II. Forty-four plasma samples from previously untreated patients diagnosed with melanoma were retrieved from the biobank of the Department of Dermatology, Essen, Germany (Study no. 19-8606-BO, 3927, 2019-373-FmB).

Cell depletions and blocking antibodies

Natural killer (NK) cells were depleted as described previously (22). Monocytes were depleted using the anti-CCR2 antibody (clone MC-21; ref. 23) and used with a Rat IgG2b isotype control (BioXCell, clone BE0090). The murine anti-PD-L1 clone 10F.9G2 (BioXCell) was used.

IHC and immunocytochemistry

Histologic analysis was performed on snap frozen tissues that were fixed in acetone, blocked with 10% FCS, and stained with anti-active caspase-3 (BD Biosciences), anti-cleaved caspase-8 (Cell Signaling Technology), anti-PD-L1, anti-LY6C, anti-LY6G (all eBioscience), and anti-BAFF (R&D) antibodies. Fluorescent images were taken with an Axiocam 503 color microscope (ZEISS) and quantified using ImageJ. Conventional histology images were taken using the Brightfield microscope.

Flow cytometry analysis

Tumors were excised, weighed, crushed, strained through a 0.45-µm filter, and surface stained with: anti-LY6G, LY6C, CD8, NK1.1, CD11b, CD45.2, F4/80, PD-L1, BAFFr, CD5, CD25, IgM, and CD19 antibodies (eBioscience). Intracellular staining for Granzyme B and IFNγ was performed using the Foxp3 mouse Treg Cell Kit (eBioscience). Experiments were performed using a FACS Fortessa and analyzed with FlowJo software.

NK cytotoxicity assays

NK-cell cytotoxicity assays were carried out as described previously (20).

Elisa

The TGFβ1 (eBioscience) and BAFF (R&D) ELISA Kits were performed according to the manufacturers' instructions.

qRT-PCR

RNA was isolated using TRIzol (Invitrogen) and RT-PCR analyses were performed using the iTaq Universal SYBR GreenOne-Step RT-qPCR Kit (Bio-Rad) or the iTaq Universal Probes One-Step Kit (Bio-Rad) according to the manufacturer's instructions. Expression levels were normalized to *Gadph*.

Lentiviral transduction and cell line generation

Lentiviral particles were generated by calcium phosphate transfection of HEK293T cells BAFF expression plasmid constructs [BAFF pLenti-C-Myc-DDK and the pLenti-C-Myc-DDK-P2A-Puro tagged open reading frame clones (Origene)]. Monoclonal cell populations were generated through clonal dilution. Polyclonal populations were puromycin selected (1.5 µg/mL of puromycin) and maintained in puromycin.

RNA sequencing and gene set analysis

RNA was isolated using TRIzol (Thermo Fisher Scientific) and 500 ng total RNA was processed using the TruSeq RNA Sample Preparation v2 Kit (low-throughput protocol; Illumina) to prepare the barcoded libraries. Libraries were validated and quantified using DNA 1000 and high-sensitivity chips on a Bioanalyzer (Agilent); 7.5 pmol/L denatured libraries were used as input into cBot (Illumina), followed by deep sequencing using HiSeq 2500 (Illumina) for 101 cycles, with an additional seven cycles for index reading. Fastq files were imported into Partek Flow (Partek Incorporated). Quality analysis and quality control were performed on all reads to assess read quality and to determine the amount of trimming required (both ends: 13 bases 5′ and 1 base 3′). Trimmed reads were aligned against the mm10 genome using the STAR v2.4.1d aligner. Unaligned reads were further processed using Bowtie 2 v2.2.5 aligner. Aligned reads were combined before quantifying the expression against the ENSEMBL (release 95) database by the Partek Expectation-Maximization algorithm using the counts per million normalization. Genes with missing values and with a mean expression less than one were filtered out. Finally, statistical gene set analysis was performed using a *t* test to determine differential expression at the gene level (*P* < 0.05, fold change ±2). Partek flow default settings were used in all analyses. Principal component analysis was performed using all genes using Covariance scaling and first three components. Data have been

publicly deposited to the NCBI GEO Database (accession no.: GSE179670).

Pathway analysis

Gene set enrichment analysis (GSEA) was performed using the *t* value from the *t* test comparing BAFF versus control tumors. Mouse gene sets were comprised of curated pathways from several databases including GO, Reactome, KEGG (August 01, 2018 version; http://download.baderlab.org/EM_Genesets/current_release/). Data were processed and visualized by using Cytoscape (www.cytoscape.org; $P \leq 0.002$, $q \leq 0.07$, similarity cutoff 0.5). Data were auto-annotated and visualized as clusters, which were manually annotated. Heatmap visualization and unsupervised hierarchical clustering was performed using all significant, differentially regulated genes from a cluster of interested after normalizing mean expression to 0 with a standard deviation of 1, and using Pearson dissimilarity algorithm and average linkage in Partek Genomics Suite (Partek Incorporated). Ingenuity pathway analysis (IPA, Qiagen) was conducted using genes with significant differential expression ($P \leq 0.05$ and fold change ± 2). The significance cut-off for IPA was set to $P \leq 0.05$ and z score of ± 1.5 for upstream regulators. In addition, for upstream regulators we filtered out biological drugs, all chemical and miRNA entries.

Data mining

The R2: Genomics Analysis and Visualization Platform (http://r2.amc.nl) was used to extract the data from TCGA for the Tumor Skin Cutaneous Melanoma cohort.

Statistical analyses

Data are expressed as mean $\pm$ SEM. Statistically significant differences were determined using the Student *t* test or the ANOVA test. For Kaplan–Meier survival curves, the log-rank test was used. Proportions were analyzed using the Fisher exact test. Values of $P < 0.05$ were considered statistically significant.

Results

Expression of BAFF in the TME inhibits tumor growth

We generated a BAFF overexpressing B16.F10 (BAFF, *Tnfsf13b*) cell line (Supplementary Figs. S1A and S1B). *In vitro*, there was no difference in growth or response to apoptotic-stimuli between the cell lines (Supplementary Figs. S1C and S1D). B16.F10 cells, when injected intravenously, will localize to the lung (24). C57BL/6 (B6) mice with control tumors succumbed faster than mice with BAFF-expressing tumors (**Fig. 1A**). For a more experimentally tractable model, we injected cells subcutaneously and, as with the intravenous model, BAFF tumors grew slower than their controls (**Fig. 1B** and **C**). Although systemic serum BAFF levels were not different between BAFF and control tumor bearing mice (Supplementary Fig. S1E), BAFF mRNA and protein expression in BAFF tumors was maintained throughout the course of tumor growth and confirmed at an early time point of tumor growth (Day 13) when there were no significant differences between tumor weight and volume, and later time point (Day 18) at sacrifice (**Fig. 1D** and **E**). To exclude any clonal selection intrinsic effects, we regenerated a polyclonal BAFF
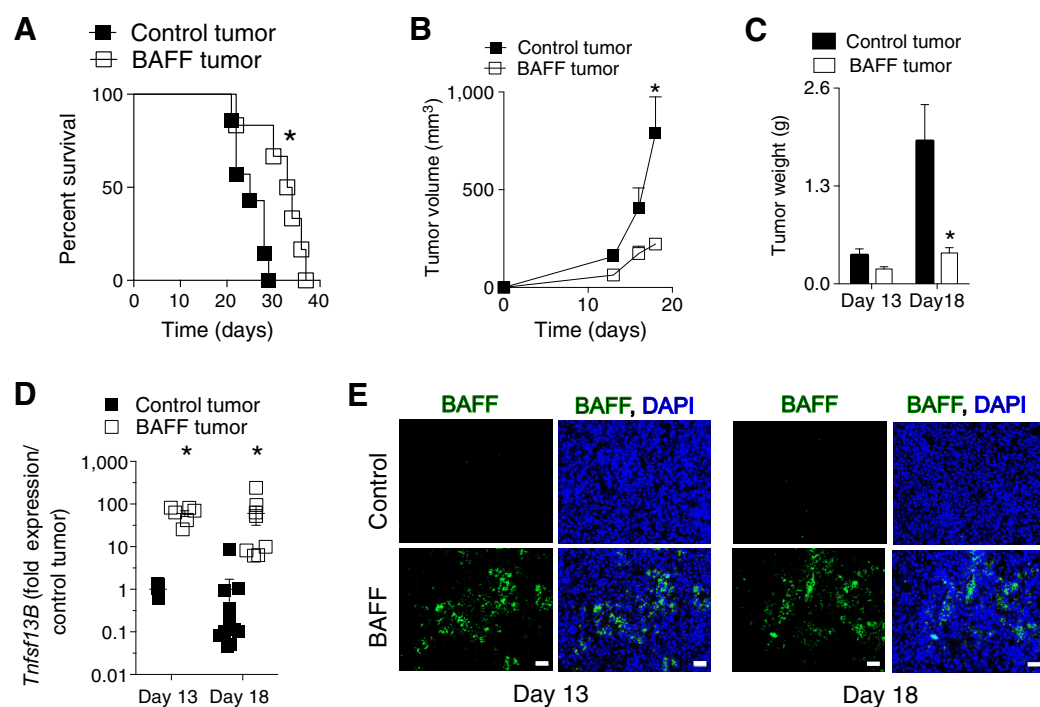
Figure 1.
Elevated BAFF in the TME slows tumor growth. **A,** C57BL/6 mice were inoculated intravenously with 10⁵ of BAFF-expressing or control cells ($n = 6-7$, pooled from two independent *in vivo* experiments). **B** and **C,** Tumor growth of 5×10^5 subcutaneously injected BAFF-expressing and control cells in C57BL/6 mice are shown ($n = 5-6$; **B**), as are tumor weights ($n = 8-10$, pooled from at least two independent *in vivo* experiments; **C**). **D,** Gene expression levels of BAFF (*Tnfsf13B*) were determined in whole tumors. Expression was normalized to *Gapdh* ($n = 5-12$, pooled from at least two independent *in vivo* experiments). **E,** BAFF protein expression was confirmed using immunohistochemical staining of tumor tissue (representative images of $n = 5-12$ mice pooled from at least two independent *in vivo* experiments are shown). Scale bar, 50 μm. Error bars in the all experiments indicate SEM. *, $P < 0.05$ as determined by a Student *t* test (unpaired, two-tailed) and log-rank test for analysis of Kaplan–Meier survival curves.

expressing cell line using an independent vector. Again, subcutaneous BAFF-expressing tumors grew slower than control tumors (Supplementary Figs. S1F and S1G). Taken together, BAFF expression within the TME delays tumor growth and prolongs survival of tumor-bearing mice, a phenomenon that is independent from intrinsic differences between the generated cell lines.
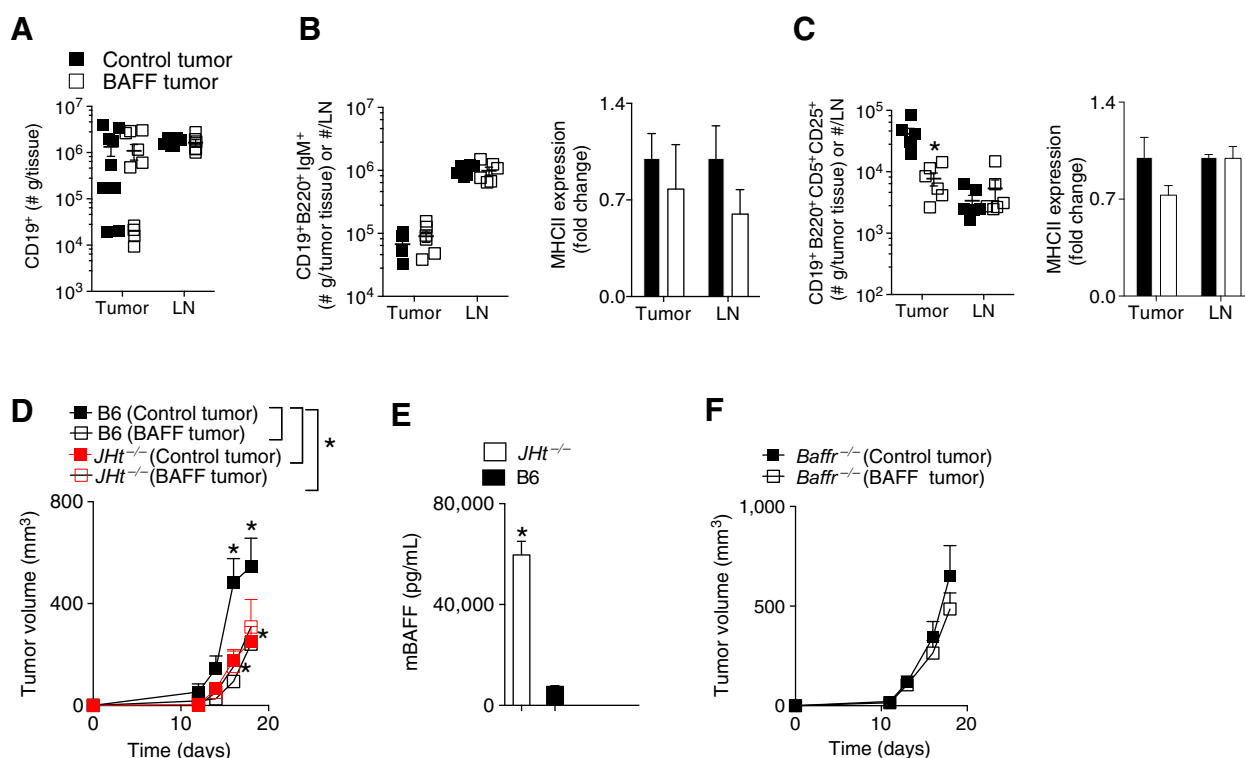
Difference in growth between BAFF and control tumors is abrogated in $JHt^{-/-}$ and $Baffr^{-/-}$ mice

As BAFF affects B cells, we wanted to test involvement of tumor infiltrating B cells within the TME. Yarchoan and colleagues showed that injection of systemic BAFF upregulated the B-cell compartment and markers of regulatory B cells including PD-L1 as well as CD5, increased Th1 responses and Tregs in the TME (19). In our system, the infiltration of CD19^{+} B cells was not significantly different in tumors and inguinal tumor draining lymph nodes between BAFF expressing and control tumors (Fig. 2A). It has been shown that certain subsets of regulatory B cells (Breg) can contribute to tumor progression (25) especially when they accumulate in tumor-draining lymph nodes (26). The infiltration and expression of MHCII on CD19^{+} B220^{+}IgM^{+} B cells was also not different in the TME and lymph node between BAFF expressing and control tumors (Fig. 2B). Although the expression of MHCII on CD19^{+} B220^{+}CD5^{+} CD25^{+} Breg's cells was not different, there was decreased infiltration of this Breg subset in the TME of BAFF-expressing tumors (Fig. 2C). The concentration of IgM and IgG within the TME was not significantly different between BAFF and

control tumors (Supplementary Fig. S2). Although the application of exogenous systemic BAFF upregulated various costimulatory molecules on B cells in the Yarchoan and colleagues study, the functional importance of B cells to tumor regression was unclear. To test this, we utilized two different B-cell defective models. In the $JHt^{-/-}$ knockout mouse model, mice lack the gene for the heavy chain joining region and therefore have no functional B cells(27). Tumor growth of both BAFF-expressing and control tumors was significantly delayed in the $JHt^{-/-}$ mice (Fig. 2D). With no B cells to take up circulating BAFF, the $JHt^{-/-}$ mice have 8-fold higher circulating BAFF levels compared with control C57BL/6J mice (Fig. 2E). In the BAFF-R deficient ($Baffr^{-/-}$) model, the mice have reduced late transitional and follicular B cells numbers and have no marginal zone B cells (28). The phenotype was abrogated in $Baffr^{-/-}$ mice (Fig. 2F). Taken together, in the absence of B cells, the phenotype was abrogated. These results imply B cell involvement and BAFF-R signaling in the observed phenotype of tumor delay upon expression of BAFF in the TME.

BAFF tumors are characterized by increased apoptosis and lower immunosuppressive factors including PD-L1

The TME is complex and characterized by many potential interactions between immune-infiltrating subsets. B cells are capable of impacting many immune subsets including innate immune cells within the TME (29). We attempted to uncover further differences between the BAFF-expressing and control tumors. When we stained tumor sections harvested at early time points, we observed increases

Figure 2.
Difference in tumor growth between BAFF and control tumors is abrogated in $JHt^{-/-}$ and $Baffr^{-/-}$ mice. C57BL/6 (B6), $JHt^{-/-}$ or $Baffr^{-/-}$ mice were inoculated subcutaneously with 5×10^5 of BAFF-expressing or control cells and tumors were analyzed as indicated on day 13 after tumor inoculation. **A,** Numbers of CD19^{+} B cells in the tumor and tumor-draining lymph node (LN) were assessed using FACS in B6 mice ($n = 6$–10). **B** and **C,** Numbers and surface MHCII expression of CD19^{+}B220^{+}IgM^{+} (**B**) and CD19^{+}B220^{+}CD5^{+}CD25^{+} (**C**) B cells in the tumor and lymph node are shown ($n = 6$). **D** and **F,** Tumor growth was analyzed in $JHt^{-/-}$ or $Baffr^{-/-}$ mice ($n = 4$–9, pooled from at least two independent *in vivo* experiments). **E,** Serum levels of BAFF in naïve B6, or $JHt^{-/-}$ mice were analyzed by ELISA ($n = 4$–5). Error bars in all experiments indicate SEM. *, $P < 0.05$ as determined by a Student *t* test (unpaired, two-tailed) or a two-way ANOVA with a *post hoc* test.

in cleaved caspase-8 and cleaved active caspase-8 and caspase-3 (**Fig. 3A**) in BAFF-expressing tumors. When we checked for perivascular heterogeneity using PDGFRβ at early time points during tumor growth, there was no difference between control and BAFF-expressing tumors (Supplementary Fig. S3A).

To further characterize the differences between BAFF-expressing and control tumors on a molecular whole-tumor level, we assayed the mRNA expression of a variety of growth factors, ligands, cytokines, and IFN responsive genes known to impact tumor growth. There was no difference between the expression of angiogenesis-related genes *Vegfa* and *Vegfb*, which is in line with what we observed for the PDGFRβ staining. The expression of immunosuppressive factors such as *Tgfb1, Il10, Pdgfb,* and *Fgf1* were significantly lower in the BAFF-expressing tumors at Day 13 after tumor injection (**Fig. 3B**). IL10 was not detectable in the tumor, and there were no significant differences in secreted TGFβ1 at the early time point between BAFF-expressing and control tumors (**Fig. 3C**), leading us to conclude that IL10 or TGFβ1 were likely not responsible for the observed phenotype. The expression of the PD-L1 was also lower in BAFF-expressing tumors (**Fig. 3B**; Supplementary Fig. S3B). PD-L1 is a crucial inhibitory ligand expressed on immune cells of the myeloid lineage, activated cells of lymphoid and epithelial origin including cancer cells (30). PD-L1 binding to PD-1 expressed on T cells decreases T-cell activation and function, therefore consequentially blunting antitumor immunity (31). When we assessed PD-L1 expression using IHC, there were differences between BAFF-expressing and control tumors (**Fig. 3D**). Next, we decided to uncover the source of the differences in PD-L1 expression. As primary human and murine tumors have been shown to express PD-L1, including those generated from B16 cells (32), we assessed PD-L1 expression in the tumor cells and stroma (CD45.2$^-$ cells). Indeed, the percentage of PD-L1 expressing CD45.2$^-$ cells in the BAFF-expressing tumors was significantly lower than in control tumors (**Fig. 3E**). As assessed by FACS analysis, PD-L1 expression was significantly lower on infiltrating CD11b$^+$LY6G^{high}LY6C^{low} granulocytes and CD11b$^+$LY6C^{high}LY6G$^-$ monocytes but not CD11b$^+$F4/80^{high}LY6C^{low}LY6G$^-$ tumor-associated macrophages (TAM) and CD19$^+$ cells (**Fig. 3F**; Supplementary Figs. S3C–S3E). Taken together, BAFF-expressing tumors were characterized by increased apoptosis and decreased expression of immunosuppressive factors including PD-L1 whose expression was decreased on tumor cells, infiltrating monocytes and granulocytes.

PD-L1 and monocytes are functionally important for BAFF-mediated reduction in tumor growth

When we stained tumor sections harvested from mice bearing BAFF-expressing or control tumors, we observed a decrease in LY6C positive cell infiltrates (**Fig. 4A**), which was corroborated using FACS analysis (**Fig. 4B**). Specifically, we saw reduction in tumor-infiltrating monocytes and TAMs but not granulocytes in BAFF-expressing tumors (**Fig. 4B**). As monocytes can transform into TAMs, their reduction in BAFF-expressing tumors alongside the monocytes was not surprising. Because we observed deceased PD-L1 expression on monocytes, we decided to focus on this population and observed that upon depletion of monocytes using an anti-CCR2 antibody this population was critical for the TME-BAFF associated phenotype (**Fig. 4C**). To confirm the functional importance of PD-L1 to BAFF-mediated repression of PD-L1 expression, we treated mice inoculated with BAFF-expressing and control cells with an anti-PD-L1 antibody and found that although the phenotype was main-

tained with control treatment, it was abrogated with anti-PD-L1 treatment (**Fig. 4D**).

As we have shown the phenotype to be dependent on BAFF-R signaling (**Fig. 2F**), we assessed the expression of BAFF-R in inflammatory monocytes. Treatment of *ex vivo* cultured inflammatory monocytes derived from the bone marrow with BAFF led to the upregulation of the BAFF-R as well as engagers of adaptive immunity MHCII, CD80, and CD86 (**Fig. 4E**). Collectively, we have demonstrated that differences in PD-L1 expression between BAFF-expressing and control tumors occur in the infiltrating monocytic populations, which are functionally critical for the maintenance of BAFF-mediated differences in tumor growth.

BAFF induces differential gene expression in tumor-infiltrating monocytes

To determine what signaling pathways are affected by BAFF in tumoral monocytes, we sorted tumor-infiltrating monocytes from early Day 13 tumors. We performed RNA-seq analysis on the sorted monocytes (Supplementary Figs. S4A and S4B). As expected, monocytes sorted from BAFF-expressing tumors were characterized by lower PD-L1 mRNA levels (Supplementary Fig. S4C). GSEA on the differentially expressed genes (Supplementary Table S1) was implemented to determine prominent pathways altered between monocytes harvested from control and BAFF-expressing tumors visualized using Cytoscape (**Fig. 5A**). Regulation of adaptive immune responses, NF-κB, and apoptosis signaling pathways was enriched in monocytes harvested from BAFF-expressing expressing tumors. In contrast, cell-cycle regulation and ECM/Collagen formation pathways were enriched in monocytes harvested from control tumors. Significant individual genes differentially regulated in regulation of adaptive immune responses, apoptosis, and NF-κB signaling pathways are represented in heatmaps (**Fig. 5B**). Genes involved in the activation of NF-κB signaling (*Tnfrs8, Adgrg3, Id1, Malt1*) were upregulated in monocytes harvested from BAFF tumors whereas negative regulators (*Traip, Gas6*) were downregulated. Fittingly, proapoptotic genes (*Fas, Tnfsf14, Tnfrsf12A*) were downregulated and pro-survival (*Mybl2, Hells, Trim2, Pik3r3*) genes were upregulated in monocytes harvested from control tumors. This is in accordance with the decreased numbers of infiltrating monocytes observed in BAFF-expressing tumors pointing to an expansion of PD-L1 positive immunosuppressive monocytes in control tumors. In addition, factors such as *Pglyrp1*, which are also cytotoxic to cancer cells, were also upregulated in monocytes from BAFF-expressing tumors (33) as were genes that positively engage the adaptive arm of the immune system, indicating a shift in proinflammatory, antitumorigenic responses, and the activation of CD8$^+$ T and NK cells. Specifically, expression of receptors and factors that activate CD8$^+$ T cells and/or NK cells *Tarm1, Cd80, Cd86, Tnfs14* (34) were upregulated on monocytes harvested from BAFF tumors. This is further supported by IPA, which showed that the top upstream regulators in monocytes from BAFF-expressing tumors were IFNγ, TNF, and IL1β (**Fig. 5C**). In contrast, cell-cycle–related genes were inactivated in BAFF-expressing tumor harvested monocytes (Supplementary Fig. S4D). Taken together, tumoral BAFF shifts the monocytic phenotype to an antitumorigenic state and curbs expansion of PD-L1 positive immunosuppressive monocytes.

NK cells are important for BAFF-triggered differences in tumor growth

As shown by the RNA-seq data, monocytes from BAFF-expressing tumors were enriched for factors activating cytotoxic lymphocyte
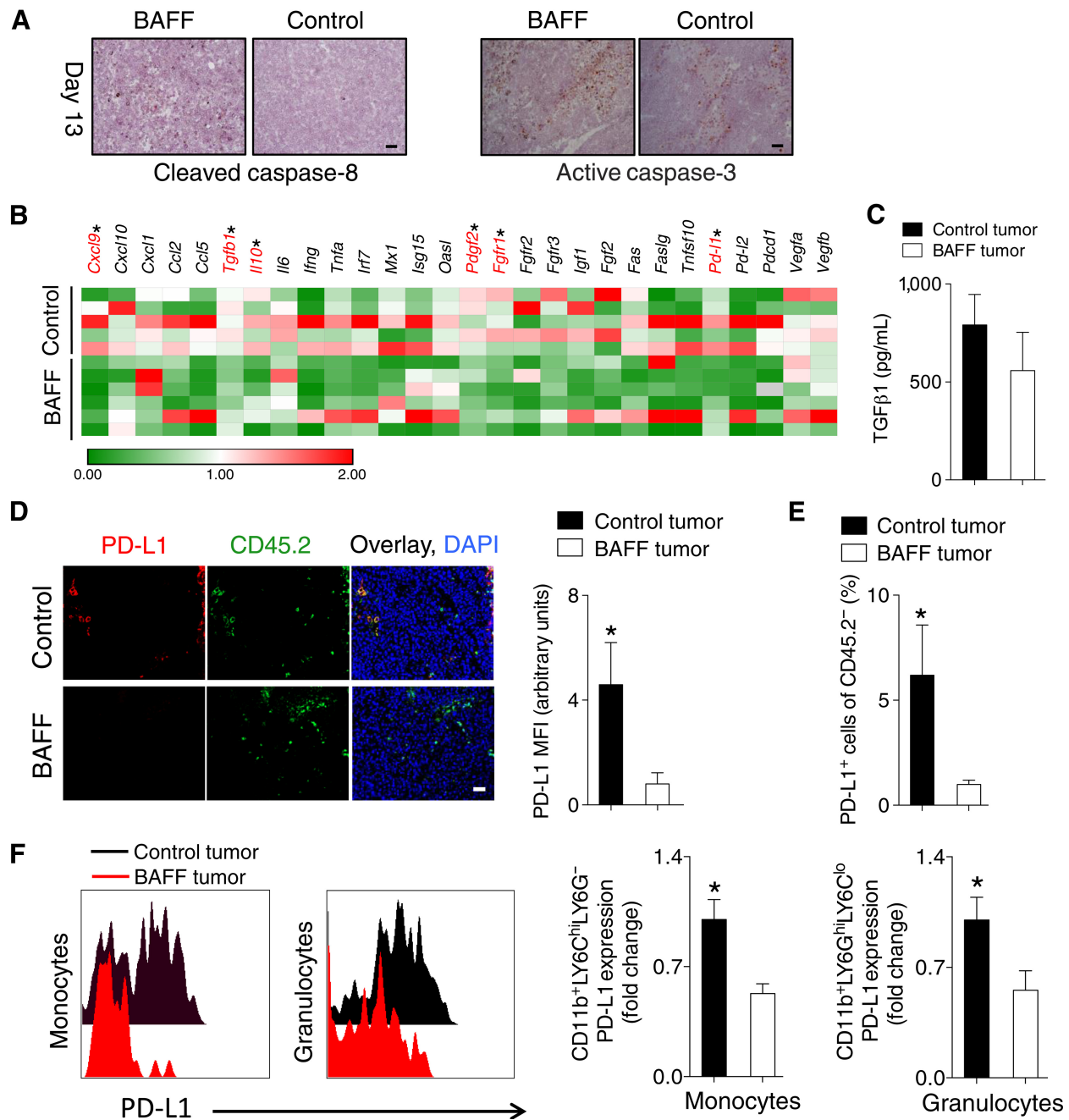
Figure 3.
BAFF tumors are characterized by increased apoptosis and decreased immunosuppressive factors including PD-L1. **A–F,** C57BL/6 mice were inoculated subcutaneously with 5×10^5 of BAFF-expressing or control cells and tumors were analyzed as indicated at day 13. **A,** Tumor apoptosis was assessed using conventional IHC staining for active caspase-3 and cleaved caspase-8 (representative images of $n = 3$–4 mice are shown). Scale bar, 50 μm. **B,** Gene expression level of various factors was determined in whole tumors. Expression was normalized to *Gapdh* and then to control tumors within each independent experiment ($n = 5$–6, pooled from two independent *in vivo* experiments). **C,** The levels of soluble TGFβ1 protein in tumors were determined using ELISA ($n = 6$–8, pooled from two independent *in vivo* experiments). **D,** PD-L1 protein expression in tumors was assessed using fluorescent IHC (a representative image of $n = 5$–6 mice from two independent experiments is shown; left) and quantified (right). **E,** Percent of PD-L1–positive CD45.2$^-$ cells in tumors was assessed using FACS ($n = 9$–10, pooled from three independent *in vivo* experiments). **F,** PD-L1 expression was measured on monocytes and granulocytes using FACS ($n = 9$–10, pooled from three independent *in vivo* experiments). All scale bars indicate 50 μm. Error bars in all experiments indicate SEM. *, $P < 0.05$ as determined by a Student t test (unpaired, two-tailed).
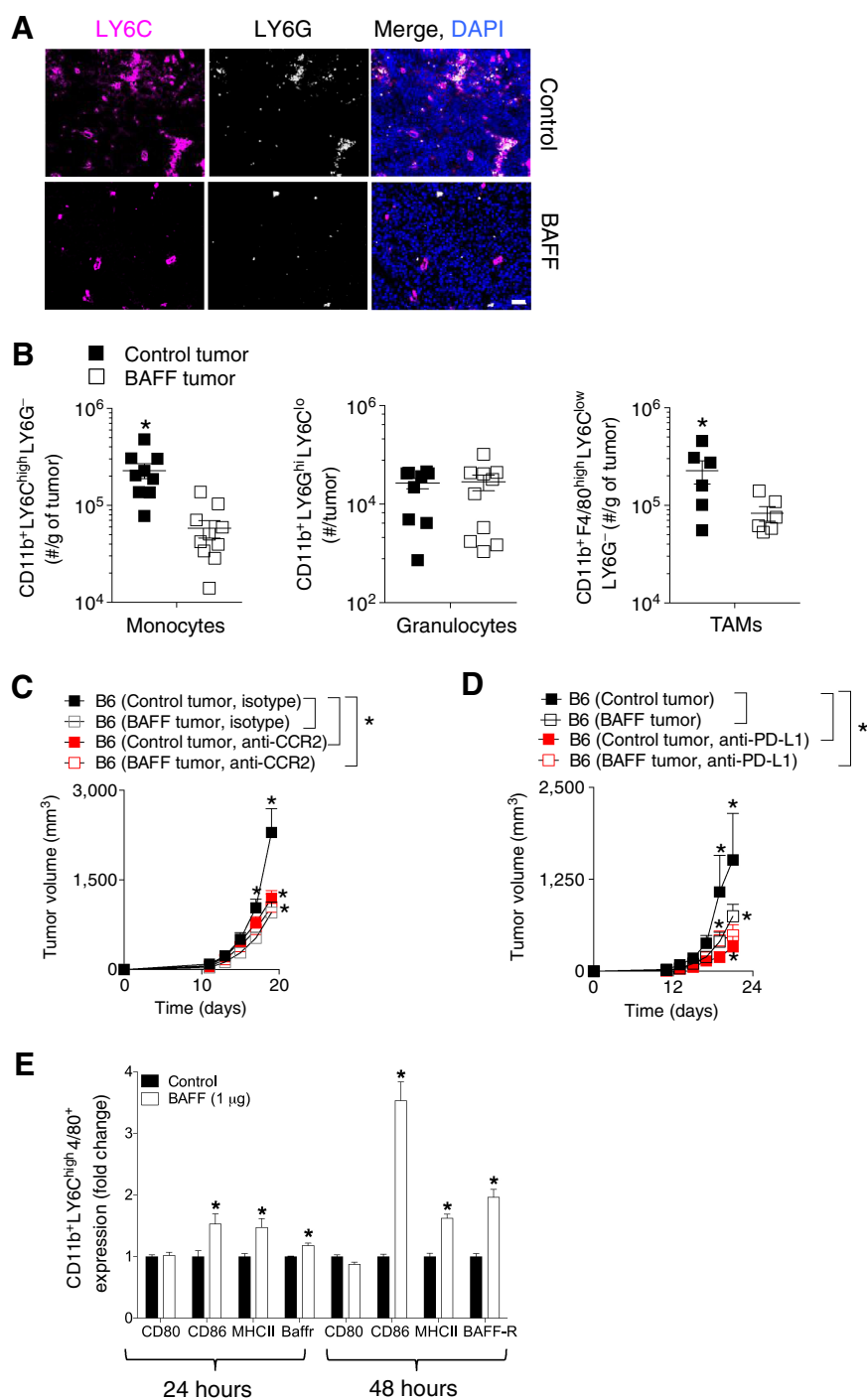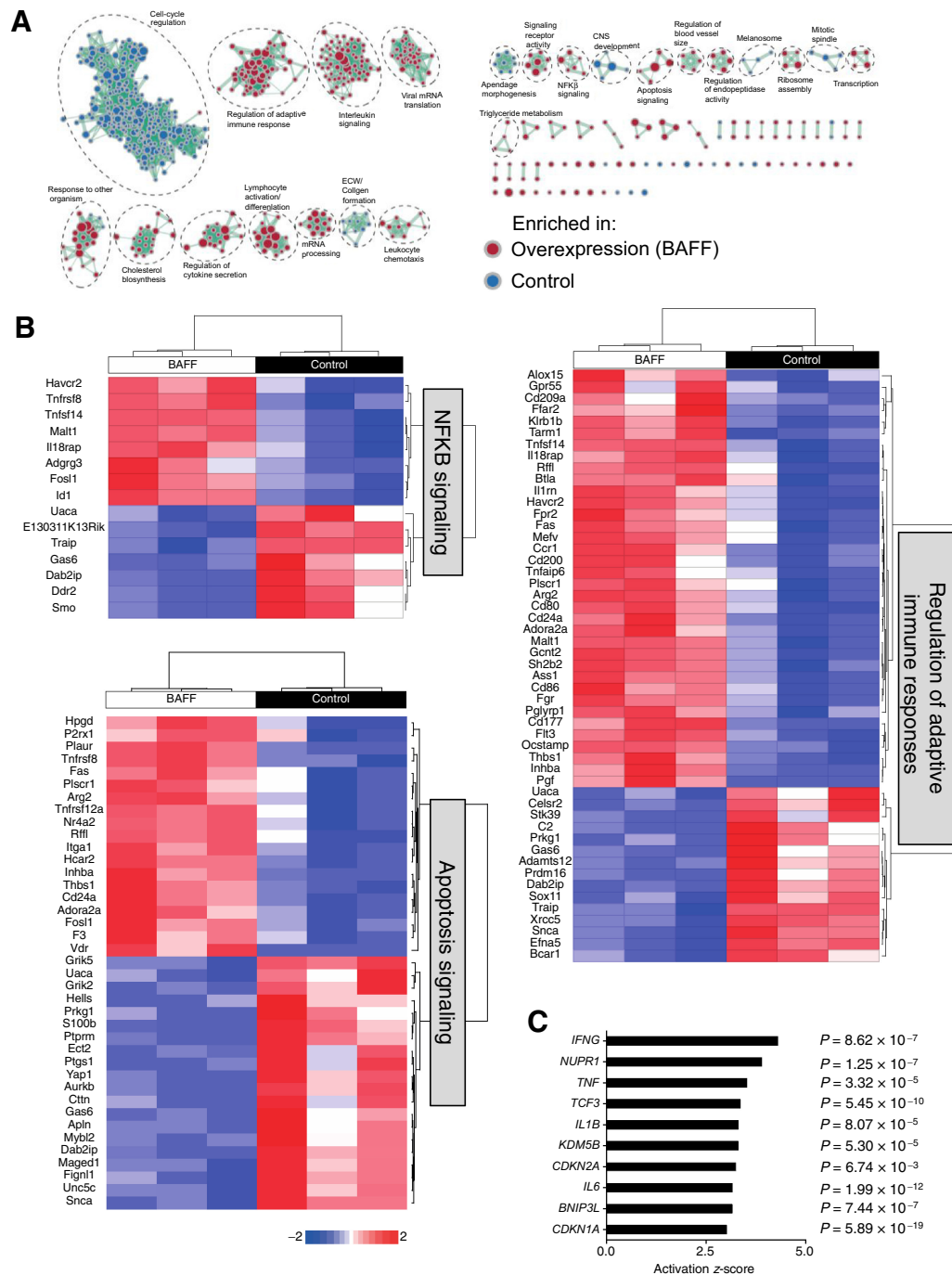
Figure 4.
PD-L1 and monocytes are functionally important for the BAFF-mediated reduction in tumor growth. **A–D**, C57BL/6 mice were inoculated subcutaneously with 5×10^5 of BAFF-expressing or control cells and tumors were analyzed as indicated at day 13. **A,** LY6C and LY6G expression in tumors was assessed using fluorescent IHC (representative images of $n = 5$–7 mice are shown). Scale bar, 50 μm. **B,** Numbers of monocyte, granulocyte, and TAMs infiltrates in tumors were analyzed using FACS ($n = 6$–10). **C,** C57BL/6 (B6) mice were treated with monocyte depleting antibody (anti-CCR2) and tumor growth was followed ($n = 7$–8, pooled from two independent *in vivo* experiments). **D,** C57BL/6 (B6) mice were treated with anti-PD-L1 antibody and tumor growth was followed ($n = 4$–5). **E,** Bone marrow–derived inflammatory monocytes were treated with 1 μg of BAFF protein for 24 hours 4 days post-isolation from the bone marrow. Expression of MHCII, CD86, CD80, and BAFF-R was analyzed using FACS ($n = 4$). Error bars in all experiments indicate SEM. *, $P < 0.05$ as determined by a Student t test (unpaired, two-tailed) or a two-way ANOVA with a *post hoc* test.

CD8$^+$ T and NK cells. We therefore wondered about the effects of BAFF on cytotoxic lymphocytes. First, we evaluated tumor infiltrating CD8$^+$ T cells using FACS analysis and found no significant differences in infiltrating CD8$^+$ T and CD8$^+$ T IFNγ producing cell numbers between BAFF-expressing and control tumors (**Fig. 6A**). Expression of surface molecule exhaustion markers PD-1 and IL7 receptor (IL7R) as well markers indicating improved T-cell immunity such as granzyme B or Eomes were also not different between CD8$^+$ T cells isolated from BAFF-expressing and control tumors

(Supplementary Fig. S5A). When mice lacking CD8 T cells ($Cd8^{-/-}$) were inoculated with BAFF-expressing and control cells, there were significant differences in tumor growth between BAFF and control tumors (**Fig. 6B**), indicating that the phenotype may mainly not be dependent on CD8$^+$ T cells. The B16.F10 cells also express the H-2Db-restricted GP33 peptide CTL epitope (residues 33 to 41 of the glycoprotein from the lymphocytic choriomeningitis virus; ref. 21). However, numbers of tetramer specific CD8$^+$ T cells in the tumor and inguinal lymph node were not different between
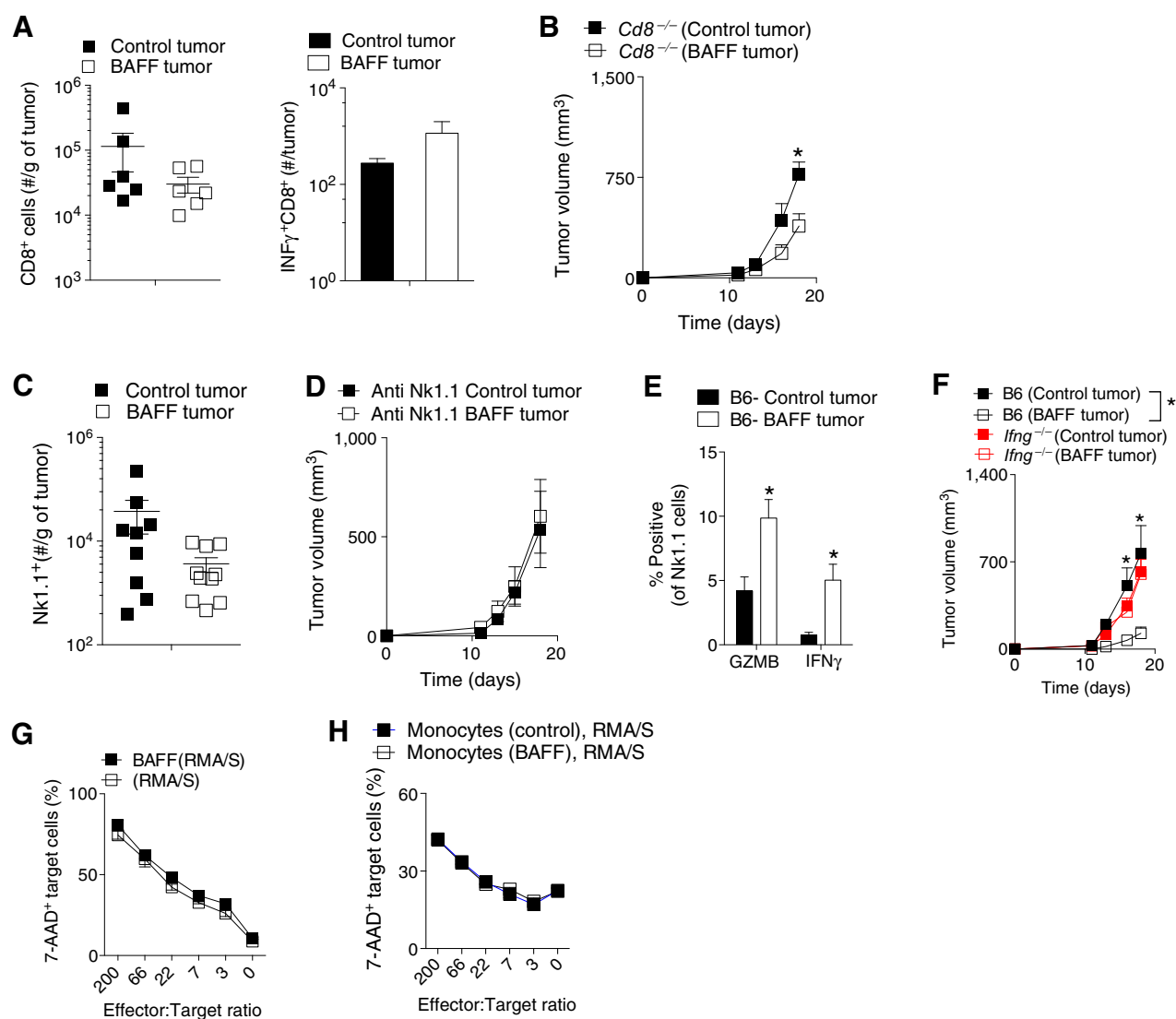
Figure 5.
BAFF induces differential gene expression in tumor-infiltrating monocytes. C57BL/6 mice were inoculated subcutaneously with 5×10^5 of BAFF-expressing or control cells. **A,** Thirteen days post-inoculation, monocytes were sorted from BAFF and control tumors, and analyzed using RNA-seq analysis for GSEA. **B,** Significant individual genes differentially regulated in regulation of adaptive immune responses, apoptosis, and NF-κB signaling pathways are shown as heatmaps. **C,** Top upstream regulators as assessed by IPA in monocytes harvested form BAFF-expressing tumors are shown ($n = 3$).

BAFF-expressing and control tumors (Supplementary Fig. S5B). Without additional stimulation, antigen presentation would not elicit strong adaptive responses in this poorly immunogenic "cold" tumor model. Depletion of CD4$^+$ T cells also maintained the phenotype (Supplementary Fig. S5C) and the infiltration of

Tregs (CD4$^+$CD25$^+$FOXP3$^+$) was not different between BAFF-expressing and control tumors within the TME (Supplementary Fig. S5D).

In addition to CD8$^+$ T cells, cytotoxic lymphocytic elimination of cancer cells can also be mediated by NK cells whose cytotoxic tumor-

Figure 6.
NK cells contribute to BAFF-triggered differences in tumor growth. **A–F,** C57BL/6 (B6) or *Ifng*$^{-/-}$ mice were inoculated subcutaneously with 5×10^5 of BAFF-expressing or control cells and tumors were analyzed 13 days post-inoculation. **A,** Left, numbers of CD8$^+$ T-cell infiltrates in BAFF and control tumors were analyzed using FACS (*n* = 6, pooled from two independent *in vivo* experiments; right) as were number of IFNγ$^+$ CD8$^+$ T cells (*n* = 4; right). **B,** Tumor growth was followed in *Cd8*$^{-/-}$ mice (*n* = 3–6). **C,** Numbers of Nk1.1$^+$ cell infiltrates in tumors were analyzed using FACS (*n* = 9–10, pooled from three independent *in vivo* experiments). **D,** Tumor growth was followed in C57BL/6 mice treated with NK-cell depleting antibody (anti-Nk1.1; *n* = 5). **E,** Granzyme B (GZMB) and IFNγ intracellular expression was measured in tumor-infiltrating Nk1.1 cells using FACS analysis at day 13 after tumor inoculation (*n* = 3–5). **F,** Tumor growth was followed in *Ifng*$^{-/-}$ and C57BL/6 (B6) mice (*n* = 5–8, pooled from two independent *in vivo* experiments). **G** and **H,** The ability of BAFF (1 μg)-treated NK cells (**G**) or NK cells combined with monocytes harvested from BAFF-expressing or control tumors (**H**) to kill RMA/S cell was measured at the indicated effector/target ratios (*n* = 3). Error bars in all experiments indicate SEM. *, *P* < 0.05 as determined by a Student *t* test (unpaired, two-tailed) or a two-way ANOVA with a *post hoc* test.

killing functions are independent of MHC-mediated antigen presentation (35,36). BAFF-expressing and control tumors were characterized by similar levels of NK infiltrates (**Fig. 6C**). However, upon depletion of NK cells, there were no difference in growth between the BAFF-expressing and control tumors (**Fig. 6D**), indicating that NK cells contribute to the observed phenotype. Intracellular staining of tumoral NK cells showed that a higher percentage of NK cells harvested from BAFF-expressing tumors expressed granzyme B and IFNγ as compared with control tumors (**Fig. 6E**). Production of the pleiotropic cytokine IFNγ, which is produced by activated lymphocytes including NK cells, has a complex, often beneficial role in

antitumor immunity and has been shown to be an effector of cytotoxic NK cells (36). When we inoculated IFNγ knockout mice (*Ifng*$^{-/-}$) with BAFF-expressing and control cells, there was no difference in tumor growth (**Fig. 6F**; Supplementary Fig. S7). There were no differences in tumoral IFNγ levels at the early time points (Supplementary Fig. S5E). Addition of BAFF to *ex vivo* cultures of NK cells did not alter their ability to kill target cells (**Fig. 6G**), indicating that the engagement of the other immune infiltrates are needed to alter their phenotype in the context of BAFF-expressing and control tumors. When we isolated monocytes from BAFF and control tumors and added them to *ex vivo* cultures of NK cells and RMA/S cells, there was also no difference in

NK-cell killing ability (**Fig. 6H**). Taken together, although NK cells contributed to the observed growth differences between BAFF-expressing and control tumors, the effects are unlikely to be mediated by a direct monocyte–NK-cell interaction but possibly involve mediator cells such as B cells.

Melanoma patients have variable BAFF levels *prior to* immunotherapy treatment

Resistance and the inability to predict response to checkpoint inhibitors has posed challenges necessitating a deeper understanding of the factors regulating PD-L1 and PD-1 (31). In melanoma, although patients expressing PD-L1 have a better prognosis, PD-L1 expression is not necessarily predictive (37).

We wondered whether patients with melanoma have higher systemic levels of BAFF as was observed in some solid tumor types (14, 16). We analyzed BAFF plasma levels in a cohort of 44 melanoma anti-PD-1 therapy naïve patients and 11 healthy volunteer controls. Baseline S100 and tumoral PD-L1 data were available for some patients

(**Fig. 7A**; Supplementary Table S2). The S100 family of proteins are intracellular calcium sensors that are often dysregulated in cancer and useful as biomarkers of prognosis, relapse, and treatment progress (38). In contrast to the patients with melanoma, which exhibited a broad range of BAFF plasma concentrations (16–6,859 pg/mL), the healthy controls had a narrower BAFF range (**Fig. 7B**). The evaluated patients with melanoma were all at advanced stages of disease namely AJCC Stage IV (defined as having by distant metastases (Supplementary Table S2) and some Stage III patients (defined as having micrometastases; ref. 39). When we compared BAFF plasma levels between the different stages, patients with a lower stage had significantly higher BAFF plasma levels than state IV patients (**Fig. 7C**). A higher stage also corresponds to an increased primary tumor thickness (39), which is in accordance to what we observed in our *in vivo* mouse models. We postulated that if elevated BAFF levels led to a decrease in PD-L1 expression, these patients might respond differently to immunotherapies as they would have already had the benefit of reduced PD-1/PD-L1 without prior immunotherapy administration. In

Figure 7.
BAFF serum levels affect response to immunotherapy. **A,** A schematic of the time line of sample collection (red) and treatment (black) of naïve melanoma patients is shown. BAFF plasma levels were assessed in healthy controls ($n = 11$) and naïve melanoma patients ($n = 44$). **B,** Patients were stratified according to their BAFF plasma levels into high and low groups. **C,** BAFF plasma levels of patients categorized according to tumor stage are shown. **D,** Best response to anti-PD-1 therapy was compared in the high and low BAFF naïve melanoma patients. **E,** Expression of tumoral BAFF mined from TCGA using the R2: Genomics Analysis and Visualization Platform was grouped by melanoma stage. **F,** BAFF expression was correlated with Breslow thickness. **G,** A model proposing effects of intratumoral BAFF on the immune infiltrates in the TME is shown. It is proposed that tumoral BAFF directly (**1**) affects monocytes or indirectly (**2**) through other immune infiltrates, mainly B cells. Error bars in all experiments indicate SEM. *, $P < 0.05$ as determined by a Student t test (unpaired, two-tailed). A Fisher exact test was used to compare proportions of responders in the high and low BAFF groups.
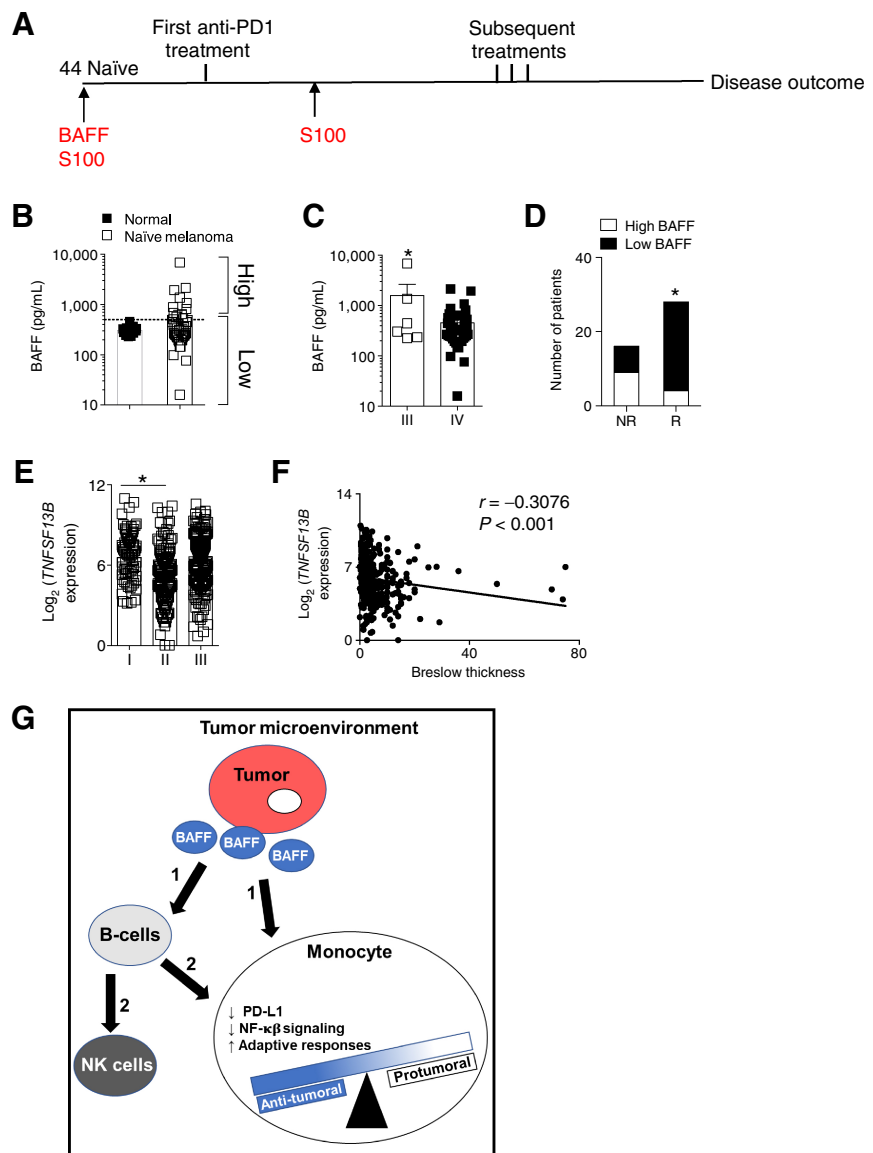
other melanoma cohorts, PD-L1 positivity ($\geq$1%) was associated with response and overall survival (OS) in checkpoint inhibitor treated patients (40) and PD-L1 expression was higher in tumor cells and macrophages of responders after 2 months of pembrolizumab/nivolumab treatment (41).

All patients in our cohort were treated with several rounds of pembrolizumab or nivolumab. When we compared responders and non-responders on the basis of BAFF or S100 concentrations, there was no significant differences between the two groups (Supplementary Fig. S6A). Given the broad range of BAFF, we were able to divide the cohort into two groups. Using control volunteer group as a reference, we stratified the melanoma patients into high BAFF (>500 pg/mL) and low BAFF cohorts ($\leq$500 pg/mL; **Fig. 7B**). Next, we analyzed the proportion of responders and patients with progressive disease following anti-PD-1 treatment. BAFF plasma levels were able to predict best overall response following several rounds of staging and multiple treatment cycles (**Fig. 7D**; **Table 1**). Although there was no difference in overall survival between the high and low BAFF groups, the patients with high BAFF plasma levels had a lower probability of progression-free survival (Supplementary Fig. S6B), which strengthens the response to immunotherapy prediction.

Rising S100 protein levels (>0.2 μg/L) have been shown to be indicative of malignant melanoma tumor progression (38, 42). We therefore wondered whether elevated BAFF levels are merely a bystander consequence of a worsening disease state. However, there were no significant differences in S100 levels between the high and low BAFF group immunotherapy naïve melanoma patients (Supplementary Fig. S6C). S100 or PD-L1 (using a 10%, 5%, and 1% cut-off) as single biomarkers were not able to identify responders to anti-PD-1 therapy (**Table 1**; Supplementary Table S3). However, this would have to evaluated with higher number of patients. A combined analysis of BAFF with the other biomarkers was also able to identify therapy responders (**Table 1**), indicating that BAFF can be combined with these two markers

to improve prediction of therapy outcome. Using the R2: Genomics Analysis and Visualization Platform (http://r2.amc.nl), we used also this cohort to confirm that higher BAFF expression was associated with a lower tumor stage and tumor thickness (**Fig. 7E** and **F**).

Discussion

BAFF plays a crucial role in antitumor immunity through its effects on immune cells within the TME, lymph nodes and systemic circulation. While the study by Yarchoan and colleagues focused on systemic BAFF and effects on B cells (19), through tumor-specific expression of BAFF within the TME, we found that monocytes were also critical to maintaining the delay in tumor growth in BAFF tumors. PD-L1 positive monocytes are crucial in maintaining an immunosuppressive, protumorigenic phenotype (32, 43–45) and exert their immunosuppressive effects through inhibition of antitumor functions of T and NK cells, secretion of immunoregulatory cytokines and presentation of surface inhibitory molecules(32, 44, 46).

Monocyte and TAM numbers were decreased in BAFF tumors, indicating that BAFF inhibited their infiltration and/or expansion within the TME, in line with proapoptotic genes being upregulated and proliferation genes being downregulated in monocytes harvested from BAFF-expressing tumors. Positive regulators of NF-κB signaling were upregulated in monocytes harvested from BAFF-expressing tumors. As NF-κB signaling occurs after binding of BAFF to the BAFF-R and *ex vivo* treatment with BAFF upregulated the BAFF-R on monocytes, we speculate that some forward signaling occurs directly through the BAFF-R on monocytes. This is supported by studies showing direct activating effects of BAFF on monocytes and cell lines (47).

Upregulation of PD-L1 in the TME is mediated by IFNγ (48), interferon receptor signaling pathways (49), by monocyte-derived IL10 (43) and TNFα (50). Although IFNγ was shown to impact the growth difference between BAFF and control tumors, it is likely not

Table 1. Evaluation of BAFF, S100, and PD-L1 as biomarkers of response to anti-PD1 therapy.

Response according to best overall response[a]: individual biomarker							
BAFF			**S100**			**PD-L1**	
	R	NR		R	NR		R	NR
Low < 500 pg/mL	24	7	Low < 0.2 μg/L	13	4	Low < 10%	19	10
High $\geq$ 500 pg/mL	4	9	High $\geq$ 0.2 μg/L	10	10	High $\geq$ 10%	3	1
Fisher *P*	0.0058		Fisher *P*	0.1734		Fisher *P*	1	
PPV	0.56		PPV	0.71		PPV	0.09	
NPV	0.86		NPV	0.57		NPV	0.86	
LR	3.07		LR	2.13		LR	0.73	

Response according to best overall response: combined biomarkers							
BAFF + PD-L1			**BAFF + S100**			**BAFF + S100+ PD-L1**	
	R	NR		R	NR		R	NR
Low	22	11	Low	21	8	Low	25	9
High[b]	0	0	High[b]	2	6	High[c]	3	7
Fisher *P*	1		Fisher *P*	0.0345		Fisher *P*	0.0225	
PPV	0		PPV	0.43		PPV	0.44	
NPV	1		NPV	0.91		NPV	0.89	
LR	1		LR	2.72		LR	2.64	

Abbreviations: NPV, negative predictive value; NR, no response [progressive disease (PD), death or MR with progression to new organ sites]; PPV, positive predictive value; R, response [complete remission (CR), partial response (PR), stable disease (SD), and mixed response (MR) with no involvement of new organ sites].
[a]Best overall response is dependent on progress of disease after multiple courses of treatment, three staging and radiological analysis.
[b]Elevated BAFF and other biomarker elevated.
[c]Any two or more biomarkers elevated.

a causative factor as there was no difference in IFNγ levels in early tumor growth. Tumoral IL10 was not detectable and there were no expression differences in interferon signaling genes and *Tnfa* within the tumor making these factors likely not responsible for the decreased monocytic and CD45.2⁻ cell PD-L1 expression in BAFF-expressing tumors. Although the contribution of other factors downregulated in BAFF tumors such as *Pdgf2* and *Fgfr1* in shaping the TME remains to be further explored, host- and tumor-derived PD-L1 expression, particularly in the myeloid compartment, is crucial in regulating antitumor immunity (51).

In our system, as NK cell depletion abolished the difference in growth between BAFF and control tumors, we can speculate that NK-mediated cytotoxicity has a functional role in the phenotype. NK cytotoxic effector function is governed by a balance between expression of NK inhibitory and activating receptors on NK cells (36). Studies have shown that monocytes can directly inhibit NK cytotoxicity through the PD-1/PD-L1 axis (52, 53) and that PD-1 plays a role in NK cell cytotoxic functions (54). In our system, *ex vivo* incubation of NK cells, monocytes, and BAFF did not lead to increased NK cytotoxicity, indicating the involvement of additional immune populations such as B cells. In our system, infiltrating B cells encounter BAFF within the TME, which could account for the subtler effects and decreased immunoregulatory activities observed when compared with the earlier Yarchoan and colleagues study (19). B cells within the tumor can shape antitumor responses (29) and the decrease of infiltrating CD19⁺B220⁺CD5⁺CD25⁺ Breg subsets in BAFF tumors and the abrogation of the phenotype in murine models lacking B suggests that this is plausible. Depending on the context, BAFF can either induce or reduce the number of Breg's (29, 55). The number of Breg's in the TME of BAFF tumors was reduced and this could account for the reduction in monocyte immunosuppression as Breg's, through cytokine secretion can suppress myeloid cells, reduce NK cytotoxicity (29) and foster an immunosuppressive environment such as the one observed in our system where increased PD-L1 was observed on myeloid and tumor cells (**Fig. 7G**). NK cells are also affected by changes in B-cell mediated intratumoral antibody production that trigger antibody-dependent cell cytotoxicity mediated by NK cells (29). While at day 13 intratumoral IgG and IgM levels were not different between BAFF and control tumors, a more detailed time-dependent analysis of the antibody repertoire might demonstrate a functional link between NK and B cells in our system.

Increasing BAFF levels within the tumor could be an attractive therapeutic option potentially realized by using BAFF as a vaccine adjuvant (19) and/or incorporation of BAFF into virus-based therapeutic vaccines or oncolytic viruses (56). Another strategy would be to trigger tumor-infiltrating cells to produce BAFF within the TME. Raising tumoral BAFF levels could be especially therapeutically relevant in the context of "cold," poorly infiltrating tumors, which are not expected to respond to immunotherapies.

At present, although there exists no single effective biomarker to predict immunotherapy response, the importance of PD-L1 expression prior to treatment, has been shown to be a critical predictor of response to PD-L1 pathway blockade in several tumor types (32, 57, 58). The potential application of systemic levels of BAFF as a biomarker of response to anti-PD-1 therapy is an intriguing possibility, which, given its technical feasibility, could be added to the already existing repertoire of suggested biomarkers (59–61). Furthermore, BAFF plasma levels could indicate the preferential use of immunotherapies that do not directly target the PD-1/PD-L1 axis such as Ipilimumab (anti-CTLA4) or that anti-PD-1/PD-L1 therapies should be used in combination with Ipilimumab as opposed to a monotherapy. However, the utility of BAFF as a biomarker of potential immunotherapy response would need to be explored across larger cohorts of patients as would the finding that patients with higher BAFF responded poorly to immunotherapy given that the presence of tumoral BAFF was beneficial in preclinical models. Perhaps primary tumors that advanced to the metastatic stage despite high BAFF might have developed highly complex immunosuppressive mechanisms rendering them less responsive to immunotherapies.

In conclusion, we have identified a role for the BAFF cytokine in the context of a cold aggressive tumor type. We have shown that BAFF decreases the numbers and the suppressive phenotype of infiltrating monocytes and as a consequence, alleviates the immunosuppressive tumor environment. Taken together, this work further highlights the important role of BAFF in antitumor immunity.

Authors' Disclosures

Authors' Contributions

W. Liu: Formal analysis, validation, investigation, visualization, methodology. **P. Stachura:** Formal analysis, validation, investigation, visualization. **H.C. Xu:** Validation, investigation, methodology. **R. Váraljai:** Formal analysis, validation. **P. Shinde:** Validation, investigation, visualization, methodology. **N. Umesh Ganesh:** Validation, investigation. **M. Mack:** Resources, writing–review and editing. **A. Van Lierop:** Resources, writing–review and editing. **A. Huang:** Investigation. **B. Sundaram:** Investigation. **K.S. Lang:** Conceptualization, writing–review and editing. **D. Picard:** Data curation, software, investigation, visualization, methodology. **U. Fischer:** Conceptualization, writing–review and editing. **M. Remke:** Conceptualization, writing–review and editing. **B. Homey:** Resources, writing–review and editing. **A. Roesch:** Conceptualization, resources, writing–review and editing. **D. Häussinger:** Conceptualization, writing–review and editing. **P.A. Lang:** Conceptualization, resources, supervision, funding acquisition, methodology, project administration, writing–review and editing. **A. Borkhardt:** Conceptualization, resources, supervision, writing–review and editing. **A.A. Pandyra:** Conceptualization, supervision, funding acquisition, validation, investigation, visualization, methodology, writing–original draft, writing–review and editing.

Acknowledgments

Note

References

1. Mackay F, Schneider P. Cracking the BAFF code. Nat Rev Immunol 2009;9: 491–502.
2. Nardelli B, Belvedere O, Roschke V, Moore PA, Olsen HS, Migone TS, et al. Synthesis and release of B-lymphocyte stimulator from myeloid cells. Blood 2001;97:198–204.
3. Novak AJ, Bram RJ, Kay NE, Jelinek DF. Aberrant expression of B-lymphocyte stimulator by B chronic lymphocytic leukemia cells: a mechanism for survival. Blood 2002;100:2973–9.
4. Lavie F, Miceli-Richard C, Quillard J, Roux S, Leclerc P, Mariette X. Expression of BAFF (BLyS) in T cells infiltrating labial salivary glands from patients with Sjogren's syndrome. J Pathol 2004;202:496–502.
5. Gorelik L, Gilbride K, Dobles M, Kalled SL, Zandman D, Scott ML. Normal B cell homeostasis requires B cell activation factor production by radiation-resistant cells. J Exp Med 2003;198:937–45.
6. Thompson JS, Bixler SA, Qian F, Vora K, Scott ML, Cachero TG, et al. BAFF-R, a newly identified TNF receptor that specifically interacts with BAFF. Science 2001;293:2108–11.
7. Gross JA, Johnston J, Mudri S, Enselman R, Dillon SR, Madden K, et al. TACI and BCMA are receptors for a TNF homologue implicated in B-cell autoimmune disease. Nature 2000;404:995–9.
8. Zhang J, Roschke V, Baker KP, Wang Z, Alarcon GS, Fessler BJ, et al. Cutting edge: a role for B lymphocyte stimulator in systemic lupus erythematosus. J Immunol 2001;166:6–10.
9. Groom J, Kalled SL, Cutler AH, Olson C, Woodcock SA, Schneider P, et al. Association of BAFF/BLyS overexpression and altered B cell differentiation with Sjogren's syndrome. J Clin Invest 2002;109:59–68.
10. Strand V, Levy RA, Cervera R, Petri MA, Birch H, Freimuth WW, et al. Improvements in health-related quality of life with belimumab, a B-lymphocyte stimulator-specific inhibitor, in patients with autoanti-body-positive systemic lupus erythematosus from the randomised controlled BLISS trials. Ann Rheum Dis 2014;73:838–44.
11. Ng LG, Sutherland AP, Newton R, Qian F, Cachero TG, Scott ML, et al. B cell-activating factor belonging to the TNF family (BAFF)-R is the principal BAFF receptor facilitating BAFF costimulation of circulating T and B cells. J Immunol 2004;173:807–17.
12. Yoshimoto K, Tanaka M, Kojima M, Setoyama Y, Kameda H, Suzuki K, et al. Regulatory mechanisms for the production of BAFF and IL-6 are impaired in monocytes of patients of primary Sjogren's syndrome. Arthritis Res Ther 2011; 13:R170.
13. Novak AJ, Grote DM, Stenson M, Ziesmer SC, Witzig TE, Habermann TM, et al. Expression of BLyS and its receptors in B-cell non-Hodgkin lymphoma: correlation with disease activity and patient outcome. Blood 2004;104:2247–53.
14. Grimaldi F, Vescini F, Tonelli V, Pistis C, Kara E, Triggiani V, et al. Exploring the possible prognostic role of B-Lymphocyte Stimulator (BLyS) in a large series of patients with neuroendocrine tumors. Endocr Metab Immune Disord Drug Targets 2018;18:618–25.
15. Pelekanou V, Kampa M, Kafousi M, Darivianaki K, Sanidas E, Tsiftsis DD, et al. Expression of TNF-superfamily members BAFF and APRIL in breast cancer: immunohistochemical study in 52 invasive ductal breast carcinomas. BMC Cancer 2008;8:76.
16. Koizumi M, Hiasa Y, Kumagi T, Yamanishi H, Azemoto N, Kobata T, et al. Increased B cell-activating factor promotes tumor invasion and metastasis in human pancreatic cancer. PLoS One 2013;8:e71367.
17. Shurin MR, Ma Y, Keskinov AA, Zhao R, Lokshin A, Agassandian M, et al. BAFF and APRIL from Activin A-treated dendritic cells upregulate the antitumor efficacy of dendritic cells in vivo. Cancer Res 2016;76:4959–69.
18. Di Carlo E, D'Antuono T, Pompa P, Giuliani R, Rosini S, Stuppia L, et al. The lack of epithelial interleukin-7 and BAFF/BLyS gene expression in prostate cancer as a possible mechanism of tumor escape from immunosurveillance. Clin Cancer Res 2009;15:2979–87.
19. Yarchoan M, Ho WJ, Mohan A, Shah Y, Vithayathil T, Leatherman J, et al. Effects of B cell-activating factor on tumor immunity. JCI Insight 2020;5.
20. Huang A, Shinde PV, Huang J, Senff T, Xu HC, Margotta C, et al. Progranulin prevents regulatory NK cell cytotoxicity against antiviral T cells. JCI Insight 2019; 4:e129856.
21. Prevost-Blondel A, Zimmermann C, Stemmer C, Kulmburg P, Rosenthal FM, Pircher H. Tumor-infiltrating lymphocytes exhibiting high ex vivo cytolytic activity fail to prevent murine melanoma tumor growth in vivo. J Immunol 1998; 161:2187–94.

22. Xu HC, Grusdat M, Pandyra AA, Polz R, Huang J, Sharma P, et al. Type I interferon protects antiviral CD8+ T cells from NK cell cytotoxicity. Immunity 2014;40:949–60.
23. Mack M, Cihak J, Simonis C, Luckow B, Proudfoot AE, Plachy J, et al. Expression and characterization of the chemokine receptors CCR2 and CCR5 in mice. J Immunol 2001;166:4697–704.
24. Liu W, Stachura P, Xu HC, Umesh Ganesh N, Cox F, Wang R, et al. Repurposing the serotonin agonist Tegaserod as an anticancer agent in melanoma: molecular mechanisms and clinical implications. J Exp Clin Cancer Res 2020;39:38.
25. Kobayashi T, Oishi K, Okamura A, Maeda S, Komuro A, Hamaguchi Y, et al. Regulatory B1a cells suppress melanoma tumor immunity via IL-10 production and inhibiting T helper type 1 cytokine production in tumor-infiltrating CD8(+) T cells. J Invest Dermatol 2019;139:1535–44.
26. Ganti SN, Albershardt TC, Iritani BM, Ruddell A. Regulatory B cells preferentially accumulate in tumor-draining lymph nodes and promote tumor growth. Sci Rep 2015;5:12255.
27. Gu H, Zou YR, Rajewsky K. Independent control of immunoglobulin switch recombination at individual switch regions evidenced through Cre-loxP-mediated gene targeting. Cell 1993;73:1155–64.
28. Sasaki Y, Casola S, Kutok JL, Rajewsky K, Schmidt-Supprian M. TNF family member B cell-activating factor (BAFF) receptor-dependent and -independent roles for BAFF in B cell physiology. J Immunol 2004;173:2245–52.
29. Sharonov GV, Serebrovskaya EO, Yuzhakova DV, Britanova OV, Chudakov DM. B cells, plasma cells and antibody repertoires in the tumour microenvironment. Nat Rev Immunol 2020;20:294–307.
30. Gibbons Johnson RM, Dong H. Functional expression of programmed death-ligand 1 (B7-H1) by immune cells and tumor cells. Front Immunol 2017;8:961.
31. Merelli B, Massi D, Cattaneo L, Mandala M. Targeting the PD1/PD-L1 axis in melanoma: biological rationale, clinical challenges and opportunities. Crit Rev Oncol Hematol 2014;89:140–65.
32. Lin H, Wei S, Hurt EM, Green MD, Zhao L, Vatan L, et al. Host expression of PD-L1 determines efficacy of PD-L1 pathway blockade-mediated tumor regression. J Clin Invest 2018;128:805–15.
33. Yashin DV, Ivanova OK, Soshnikova NV, Sheludchenkov AA, Romanova EA, Dukhanina EA, et al. Tag7 (PGLYRP1) in complex with Hsp70 induces alternative cytotoxic processes in tumor cells via TNFR1 receptor. J Biol Chem 2015;290:21724–31.
34. Chen L, Flies DB. Molecular mechanisms of T cell co-stimulation and co-inhibition. Nat Rev Immunol 2013;13:227–42.
35. Martinez-Lostao L, Anel A, Pardo J. How do cytotoxic lymphocytes kill cancer cells? Clin Cancer Res 2015;21:5047–56.
36. Lopez-Soto A, Gonzalez S, Smyth MJ, Galluzzi L. Control of metastasis by NK cells. Cancer Cell 2017;32:135–54.
37. Taube JM, Klein A, Brahmer JR, Xu H, Pan X, Kim JH, et al. Association of PD-1, PD-1 ligands, and other features of the tumor immune microenvironment with response to anti-PD-1 therapy. Clin Cancer Res 2014;20:5064–74.
38. Harpio R, Einarsson R. S100 proteins as cancer biomarkers with focus on S100B in malignant melanoma. Clin Biochem 2004;37:512–8.
39. Balch CM, Gershenwald JE, Soong SJ, Thompson JF, Atkins MB, Byrd DR, et al. Final version of 2009 AJCC melanoma staging and classification. J Clin Oncol 2009;27:6199–206.
40. Morrison C, Pabla S, Conroy JM, Nesline MK, Glenn ST, Dressman D, et al. Predicting response to checkpoint inhibitors in melanoma beyond PD-L1 and mutational burden. J Immunother Cancer 2018;6:32.
41. Vilain RE, Menzies AM, Wilmott JS, Kakavand H, Madore J, Guminski A, et al. Dynamic changes in PD-L1 expression and immune infiltrates early during treatment predict response to PD-1 blockade in melanoma. Clin Cancer Res 2017;23:5024–33.
42. Jury CS, McAllister EJ, MacKie RM. Rising levels of serum S100 protein precede other evidence of disease progression in patients with malignant melanoma. Br J Dermatol 2000;143:269–74.
43. Kuang DM, Zhao Q, Peng C, Xu J, Zhang JP, Wu C, et al. Activated monocytes in peritumoral stroma of hepatocellular carcinoma foster immune privilege and disease progression through PD-L1. J Exp Med 2009;206:1327–37.
44. Fleming V, Hu X, Weller C, Weber R, Groth C, Riester Z, et al. Melanoma extracellular vesicles generate immunosuppressive myeloid cells by upregulating PD-L1 via TLR4 signaling. Cancer Res 2019;79:4715–28.
45. Witkowski MT, Dolgalev I, Evensen NA, Ma C, Chambers T, Roberts KG, et al. Extensive remodeling of the immune microenvironment in B cell acute lymphoblastic leukemia. Cancer Cell 2020;37:867–82.

46. Cane S, Ugel S, Trovato R, Marigo I, De Sanctis F, Sartoris S, et al. The endless Saga of monocyte diversity. Front Immunol 2019;10:1786.

47. Chang SK, Arendt BK, Darce JR, Wu X, Jelinek DF. A role for BLyS in the activation of innate immune cells. Blood 2006;108:2687–94.

48. Spranger S, Spaapen RM, Zha Y, Williams J, Meng Y, Ha TT, et al. Up-regulation of PD-L1, IDO, and T(regs) in the melanoma tumor microenvironment is driven by CD8(+) T cells. Sci Transl Med 2013;5:200ra116.

49. Garcia-Diaz A, Shin DS, Moreno BH, Saco J, Escuin-Ordinas H, Rodriguez GA, et al. Interferon receptor signaling pathways regulating PD-L1 and PD-L2 expression. Cell Rep 2017;19:1189–201.

50. Hartley G, Regan D, Guth A, Dow S. Regulation of PD-L1 expression on murine tumor-associated monocytes and macrophages by locally produced TNF-alpha. Cancer Immunol Immunother 2017;66:523–35.

51. Tang F, Zheng P. Tumor cells versus host immune cells: whose PD-L1 contributes to PD-1/PD-L1 blockade mediated cancer immunotherapy? Cell Biosci 2018;8:34.

52. Vari F, Arpon D, Keane C, Hertzberg MS, Talaulikar D, Jain S, et al. Immune evasion via PD-1/PD-L1 on NK cells and monocyte/macrophages is more prominent in Hodgkin lymphoma than DLBCL. Blood 2018;131:1809–19.

53. Veglia F, Perego M, Gabrilovich D. Myeloid-derived suppressor cells coming of age. Nat Immunol 2018;19:108–19.

54. Oyer JL, Gitto SB, Altomare DA, Copik AJ. PD-L1 blockade enhances anti-tumor efficacy of NK cells. Oncoimmunology 2018;7:e1509819.

55. Matsushita T, Kobayashi T, Mizumaki K, Kano M, Sawada T, Tennichi M, et al. BAFF inhibition attenuates fibrosis in scleroderma by modulating the regulatory and effector B cell balance. Sci Adv 2018;4:eaas9944.

56. Wu CC, Wu FC, Hsu YT, Hsiao YC, Yang YC, Chang CA, et al. Enhanced anti-tumor therapeutic efficacy of DNA vaccine by fusing the E7 gene to BAFF in treating human papillomavirus-associated cancer. Oncotarget 2017; 8:33024–36.

57. Herbst RS, Soria J-C, Kowanetz M, Fine GD, Hamid O, Gordon MS, et al. Predictive correlates of response to the anti-PD-L1 antibody MPDL3280A in cancer patients. Nature 2014;515:563–7.

58. Herbst RS, Baas P, Kim DW, Felip E, Perez-Gracia JL, Han JY, et al. Pembrolizumab versus docetaxel for previously treated, PD-L1-positive, advanced non-small-cell lung cancer (KEYNOTE-010): a randomised controlled trial. Lancet 2016;387:1540–50.

59. Hugo W, Zaretsky JM, Sun L, Song C, Moreno BH, Hu-Lieskovan S, et al. Genomic and transcriptomic features of response to anti-PD-1 therapy in metastatic melanoma. Cell 2016;165:35–44.

60. Huang AC, Postow MA, Orlowski RJ, Mick R, Bengsch B, Manne S, et al. T-cell invigoration to tumour burden ratio associated with anti-PD-1 response. Nature 2017;545:60–5.

61. McGranahan N, Furness AJ, Rosenthal R, Ramskov S, Lyngaa R, Saini SK, et al. Clonal neoantigens elicit T cell immunoreactivity and sensitivity to immune checkpoint blockade. Science 2016;351:1463–9.